Chemical Engineering Journal 251 (2014) 293–303

Contents lists available at ScienceDirect

Chemical Engineering Journal

journal homepage: www.elsevier.com/locate/cej

Performance of polyethyleneimine–silica adsorbent for post-combustion CO_2 capture in a bubbling fluidized bed

Wenbin Zhang, Hao Liu *, Chenggong Sun *, Trevor C. Drage, Colin E. Snape

Faculty of Engineering, University of Nottingham, University Park, Nottingham NG7 2RD, UK

HIGHLIGHTS

- CO_2 capture by PEI–silica adsorbent investigated using a kg-sorbent-scale BFB.
- CO_2 capture conducted with simulated coal-fired and NGCC flue gases.
- Equilibrium capacities stabilized at *ca.* 11 wt% for 60 cycles under humid condition.
- Heat of adsorption determined by energy balance in the fluidized bed and DSC/TGA.
- Regeneration heat for the PEI–silica adsorbent noticeably lower than MEA process.

ARTICLE INFO

Article history:
Received 22 February 2014
Received in revised form 14 April 2014
Accepted 16 April 2014
Available online 24 April 2014

Keywords:
Carbon capture
PEI
Solid adsorbent
Bubbling fluidized bed

ABSTRACT

The high performance of polyethyleneimine (PEI)-based solid adsorbent for CO_2 capture has been well recognized in thermogravimetric analysis (TGA) and small-scale fixed bed reactors through the measurements of their equilibrium capacities but has not been really demonstrated on larger scales towards practical utilization. In the present study, a laboratory-scale bubbling fluidized bed reactor loaded with a few kg adsorbent is used to evaluate the adsorption performance of PEI–silica adsorbent under different working conditions including with/without the presence of moisture, different gas–solid contact times, initial bed temperatures, and CO_2 partial pressures. The adsorption capacities have shown a clear degradation tendency under dry condition. However, they can be stabilized at a high level of 10.6–11.1% w/w over 60 cycles if moisture (*ca.* 8.8 vol%) is present in the gas flow during adsorption and desorption. Breakthrough capacities can be stabilized at the level of 7.6–8.2% w/w with the gas–solid contact time of 13 s. The adsorption capacities for the simulated flue gases containing 5% CO_2 are only slightly lower than those for the simulated flue gases containing 15% CO_2, indicating that the PEI–silica adsorbent is suitable for CO_2 capture from flue gases of both coal-fired and natural gas-fired combined cycle power plants. The exothermal heat of adsorption is estimated by the energy balance in the fluidized bed reactor and found to be close (within 10%) to the measured value by TG-DSC. The regeneration heat for the as-prepared PEI–silica adsorbent is found to be 2360 kJ/kgCO_2 assuming 75% recovery of sensible heat which is well below the values of 3900–4500 kJ/kgCO_2 for a typical MEA scrubbing process with 90% recovery of sensible heat.

1. Introduction

According to International Energy Agency [1], '*the world is not on track to meet the target agreed by governments to limit the long-term rise in the average global temperature to 2 degrees Celsius (°C). Global greenhouse-gas emissions are increasing rapidly and, in May 2013, carbon-dioxide (CO_2) levels in the atmosphere exceeded 400 parts per million for the first time in several hundred millennia*'. Fossil fuels currently supply over 80% of the world's primary energy needs and are expected to continue to supply most of the world's energy in the coming decades [2]. Combustion of fossil fuels is the major source of anthropogenic carbon dioxide that is causing the continual increase in CO_2 concentration in the atmosphere. Carbon Capture and Storage (CCS) is a process to capture carbon dioxide (CO_2) that would otherwise be emitted to the atmosphere by large point sources such as fossil fuel power stations, to transport the captured CO_2 to the storage site and permanently store the CO_2 deep underground. CCS has been considered as one potential short-medium solution that allows the continual use of fossil

* Corresponding authors. Tel.: +44 115 8467674 (H. Liu). Tel.: +44 115 7484577 (C. Sun).
E-mail addresses: liu.hao@nottingham.ac.uk (H. Liu), cheng-gong.sun@nottingham.ac.uk (C. Sun).

http://dx.doi.org/10.1016/j.cej.2014.04.063
1385-8947/

fuels without causing rapid increase in CO_2 concentration in the atmosphere.

Aqueous amine scrubbing is the most mature post-combustion CO_2 capture technology that has been commercially utilized. However, this technology suffers from the problems associated with its high regeneration cost, equipment corrosion and amine oxidative degradation and evaporation. Currently, a great deal of efforts have been made on the development of solid sorbents for post-combustion capture (PCC) due to their advantages in lower regeneration heat requirement, less amine evaporation and less vessel corrosion. These sorbents include the physi-sorbents such as zeolites [3–5] and activated carbons [6,7] and more recently chemi-sorbents such as regenerable alkaline-based adsorbents, amine-functionalized mesoporous silicas [8–11] and metal organic frameworks (MOFs) [12,13]. A number of amine-based solid sorbents have demonstrated their high adsorption efficiency and regenerability for the removal of CO_2 from flue gas mixtures [14–18]. The calcium looping technology using carbonation–calcination route, which is regarded as an alternative method to capture CO_2 from flue gas, has also attracted a lot of interests due to the advantages in its ability of high-grade heat recovery from the carbonation reaction and the wide availability and low cost of the adsorbent [19–22]. With regard to post-combustion CO_2 capture (PCC), amine based sorbents have been demonstrated more promising than physi-sorbents such as activated carbon and fly ash in terms of fast reaction kinetics, high adsorption capacity and favourable operating temperature window.

The main research methodology on characterizing amine-based solid sorbents is mostly limited to a very small amount of sorbents tested under well controlled experimental conditions using a small laboratory-scale fixed bed device such as thermogravimetric analysis (TGA), mass spectrometer (MS) or temperature programmed desorption (TPD) [14–16,18]. These investigations have focused on the equilibrium CO_2 adsorption capacities as an evaluation criterion for the performance of a specific adsorbent. However, from practical perspective, working capacities such as breakthrough capacities are more process-relevant and thus are more suitable to be used as performance indicators for a practical capture process. In addition, applying the adsorbents to practical and commercial applications also requires comprehensive knowledge on the durability and stability of the adsorbents. Fluidized bed reactors are regarded as one of the most suitable types of reactors for both the adsorber and desorber of a solid adsorbent based post-combustion capture system due to their inherent advantages in rapid particle mixing, compactness and uniform temperature distributions [23]. However, only few researchers have evaluated amine-based solid sorbents in fluidized bed reactors [24,25]. This paper reports the results of evaluation of a polyethyleneimine (PEI)-based adsorbent impregnated on a mesoporous silica support for CO_2 capture in a laboratory-scale fluidized bed reactor with simulated flue gases. The fluidized bed reactor was operated under different working conditions where the effects of presence of moisture, gas–solid contact time, initial bed temperature, and CO_2 partial pressure on the adsorption equilibrium and breakthrough capacities were investigated. Theoretical analysis on the regeneration energy penalty for the as-prepared PEI–silica adsorbent is also performed and compared to that of a typical MEA scrubbing technology. The obtained results are essential for optimization of a practical process design for post-combustion carbon capture of flue gases using the solid adsorbent.

2. Experimental

2.1. Bubbling fluidized bed (BFB) reactor

Fig. 1 illustrates a bubbling fluidized bed (BFB) reactor designed and manufactured for the purpose of CO_2 capture from simulated flue gas mixtures using low-medium temperature solid adsorbents and also for the regeneration of the adsorbents. The BFB reactor has a total height of around 1700 mm, consisting of a fluidized bed section of 1200 mm in height and 67 mm in diameter and a freeboard section of 500 mm in height and 108 mm in diameter. It is surrounded by four individually controlled electric heating elements for heating the reactor up to the required adsorption and desorption temperatures. A sintered porous stainless steel plate is

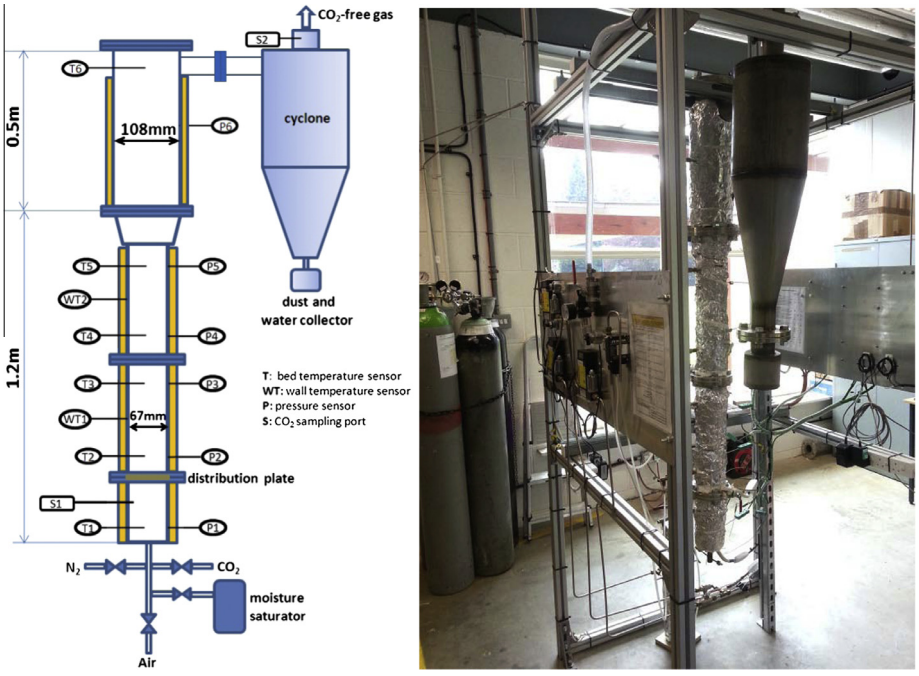

Fig. 1. Schematic and a photograph of the bubbling fluidized bed reactor.

installed and served as the gas distributor. A series of thermocouples and pressure sensors are installed on the reactor wall at different heights in order to monitor the fluidization and reaction behaviours. At the exit of the BFB, a cyclone is used to capture fine particles entrained by the flue/stripping gas before it is released to the atmosphere. At the bottom of the BFB, three gas streams i.e. air, carbon dioxide and nitrogen with individual valves and mass flow controllers are regulated to serve as the simulated flue gas for adsorption or stripping gas for regeneration for different research purposes. An electrically heated moisture saturator with separate temperature controls is used to generate the moisture for the simulated flue gas or the stripping gas. The solid adsorbent to be evaluated is loaded into the BFB as the bed material and is fluidized by the gas mixture. CO_2 concentrations (on a dry basis) at the inlet and outlet of BFB are sampled and monitored continuously by a multiple gas analyzer.

The adsorbent used in this study was synthesised by impregnating a mass ratio of 40% PEI (polyethyleneimine) into an inorganic mesoporous silica support which has a BET surface area of approximately 250 m^2/g, pore volumes of 1.7 cc/g and a mean pore diameter of approximately 20 nm [9]. The PEI has a molecular mass (MM) of 1800 in hyperbranched forms supplied by Sigma–Aldrich, UK. It was incorporated into the silica support by a wet impregnation method. Characterization of the adsorbent by TGA, NMR, DRIFT and XPS can be found in previous publications [9,26].

2.2. Experimental conditions

Cyclic performance of PEI–silica adsorbent is evaluated by measuring its capacity in CO_2 adsorption over a number of cycles of adsorption and desorption. The adsorption and desorption of the adsorbent are realized by a typical process of Temperature Swing Adsorption (TSA). The PEI–silica adsorbent bed is first preheated to the required adsorption temperature when pure N_2 is fed into the bed as protective and fluidization gas. The simulated flue gas mixture is then switched on to start the adsorption process. After the adsorption process is finished, the bed is then heated to the desorption temperature and the previously adsorbed CO_2 is desorbed during this stage to regenerate the adsorbent. Pure N_2 with or without the addition of moisture is used as the stripping gas in the desorption process. It should be noted that, to get high purity CO_2 product in practical scale application, pure CO_2 should be used as the stripping gas during the regeneration, however, this may cause serious thermal degradation and lower working capacity [9,25]. Using some portion of steam in the stripping gas can prevent the PEI–silica adsorbent from thermal degradation at the high desorption temperature, as has been demonstrated by previous investigations [11,27,28]. 100% steam was also suggested as the stripping gas by some researchers [9,16,28] to alleviate the problem but at the cost of more thermal energy penalty and additional water management. As there is no comprehensive research that has been reported up to date on the optimization of regeneration strategies including the composition of the stripping gas, this will be the focus of our research activities on PEI–silica adsorbent in the near future.

The working conditions for both adsorption and desorption tests are detailed in Table 1.

The working conditions were designed for various research purposes. Cycles of adsorption and desorption under dry or humid conditions were carried out to clarify the effect of moisture on stability of adsorption capacities. Two quantities of loaded adsorbent, Batch I and Batch II, were tested so that the impact of gas–solid contact time on the breakthrough capacities could be revealed. Effects of different adsorption temperatures and different CO_2 partial pressures on the adsorption capacities were also investigated.

Table 1
Working conditions for adsorption and desorption tests.

Adsorption	
Mass of PEI–silica adsorbent in bed (kg)	Batch I: 1.0 or Batch II: 1.9
CO_2 concentration (vol%, dry basis)	15 or 5
O_2 concentration (vol%, dry basis)	If added, 4 or 12
Moisture concentration (vol%, wet basis)	If added, saturated at 40 °C (*ca.* 8.8 vol%)
Simulated flue gas flow rate (l/min, 20 °C, 1.013×10^5 Pa)	8
Initial bed temperature (°C)	50 or 70
Desorption	
Stripping N_2 flow rate (l/min, 20 °C, 1.013×10^5 Pa)	8
Desorption temperature (°C)	130
Moisture concentration (vol%, wet basis)	If added, saturated at 40 °C (*ca.* 8.8 vol%)

3. Results and discussion

3.1. Fluidization of PEI–silica adsorbent

Fluidization tests of PEI–silica adsorbent were first carried out with air to investigate its fluidization behaviour. The results have shown that the fluidization behaviour falls into the category of Geldart B group particles based on the observation that smooth bubbles appeared once the minimum fluidization condition was achieved. Fig. 2 shows the variation of the bed pressure drop with the fluidizing air flow rate. The pressure drop increased linearly with the air flow rate when the bed was static and then levelled off irrespective of further increase in the air flow rate after the bed had already been fluidized. The transition point between static bed and fluidized bed corresponds to the minimum fluidization condition where the air flow rate was found to be around 2 l/min. As shown in Table 1, during the adsorption and desorption tests of this study, a gas flow rate of 8 l/min (at 20 °C, 1.013×10^5 Pa) was adopted which is about 4 times of the air flow rate (at 20 °C, 1.013×10^5 Pa) under the minimum fluidization condition, to ensure a fairly intensive bubbling fluidization for efficient mass and heat transfer.

The mechanical strength and attrition resistance of a specific adsorbent are two key factors that need to be considered for practical applications, especially in a fluidized bed reactor where collisions between solids–solids and solids–walls happen all the time. Weak and fragile adsorbent particles are easy to break into fines.

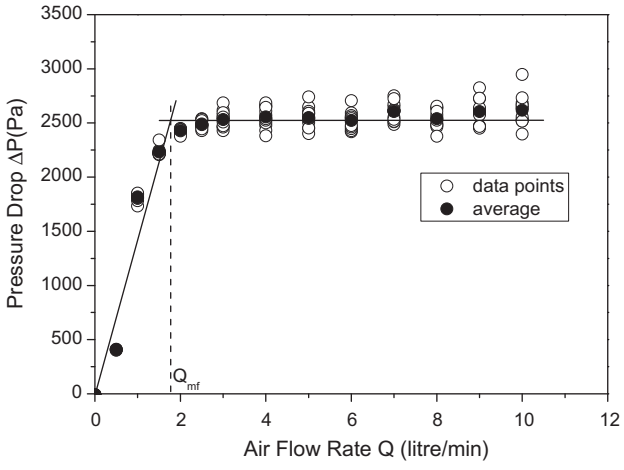

Fig. 2. Fluidization behaviour of PEI–silica adsorbent in the BFB reactor.

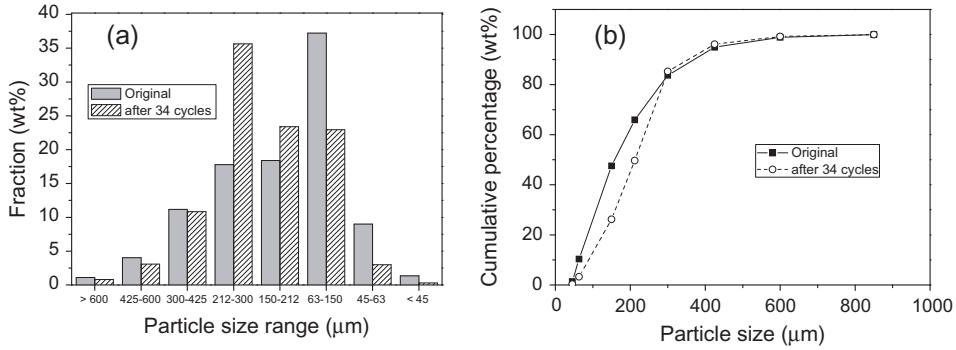

Fig. 3. Comparison of (a) fractional and (b) cumulative particle size distribution of the original PEI–silica adsorbent and that after 34 cycles of tests (Batch I, no added moisture in the simulated flue gas or the stripping gas).

An increased entrainment of fines out of the bed will increase the top-up rate of adsorbent and thus result in higher operational cost. Fractional and cumulative particle size distributions of the original PEI–silica adsorbent and those subjected to 34 dry cycles of tests have been determined by the standard sieve analysis and were displayed in Fig. 3. For the as-prepared original PEI–silica adsorbent, the average particle size was about 250 μm with the fraction of 63–150 μm being the largest portion. The fine particle fraction with the diameter less than 63 μm was about 10.3 wt%. After 34 cycles of tests, however, the weight fraction of this group of fine particles was reduced to 3.3 wt%. This implies that entrainment of fine particles originally present in the as-received adsorbent occurred. The observation of the particles caught by the cyclone also indicated that the greatest loss of the fines happened only in the first several cycles. The relatively constant bed mass after the initial cycles measured during the subsequent cycles confirmed that there was an insignificant quantity of fine particles newly generated due to attrition and collision, indicating a good mechanical character of the PEI–silica adsorbent. It can also be found in Fig. 3 that after 34 cycles, the largest fraction of particles had moved from 63–150 μm group to 212–300 μm group, resulting in an increase in the average particle size. This is likely due to the agglomeration of particles prompted by the sticky amine-related products formed on the surface of PEI–silica particles as a result of thermal degradation and evaporation under the relatively high desorption temperature used (130 °C). Fig. 4 shows the comparison of SEM images taken for the original PEI–silica adsorbent and the adsorbent subjected to 20 dry cycles of adsorption/desorption. Figs. 4(a) and (b) with 400× magnification indicate an average particle size increment in the visual field after 20 dry cycles; Figs. 4(c) and (d) with 2000× magnification show the appearance of an individual PEI–silica particle while Figs. 4(e) and (f) with 8000× magnification clearly detail the surface morphology which illustrates growing aggregates on the surface of PEI–silica particle after 20 dry cycles of tests.

3.2. Cyclic adsorption and desorption tests

Fig. 5 plots the profiles of CO_2 concentration and bed temperature with time during adsorption and desorption stages for a typical cycle when Batch II PEI–silica adsorbent was used for CO_2 capture tests. At the initial stage of adsorption, all CO_2 contained in the simulated flue gas was adsorbed by the PEI–silica adsorbent therefore no CO_2 has been detected at the exit of the bed, indicating 100% capture efficiency. This stage lasted for about 65 min until 10% of the input CO_2 in the simulated flue gas can be detected, at which point the breakthrough condition is defined in this study, corresponding to a capture rate of 90%, as adopted by most

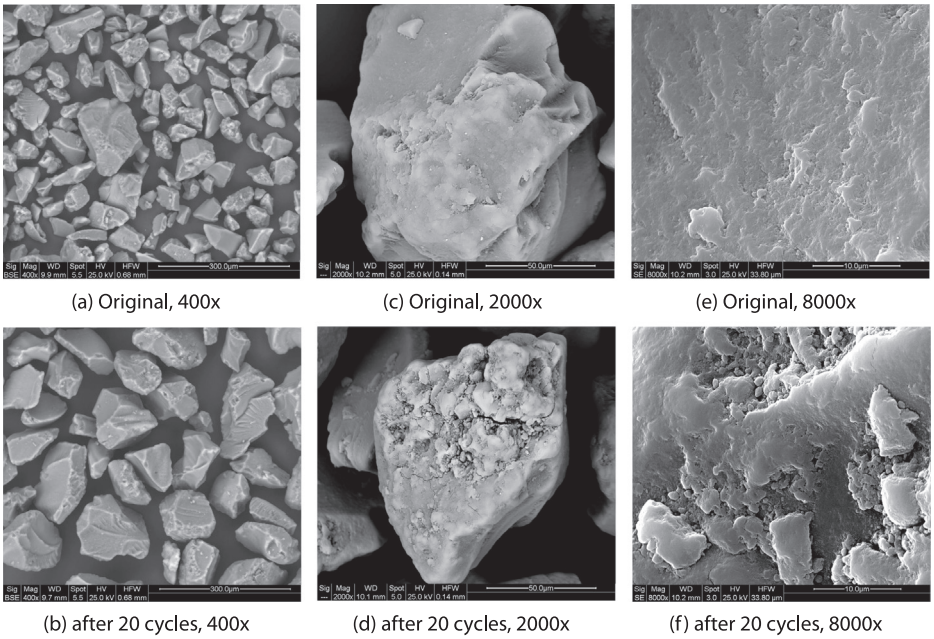

Fig. 4. SEM images of original PEI–silica adsorbent and the adsorbent subjected to 20 dry cycles of tests with three magnifications 400×, 2000× and 8000×.

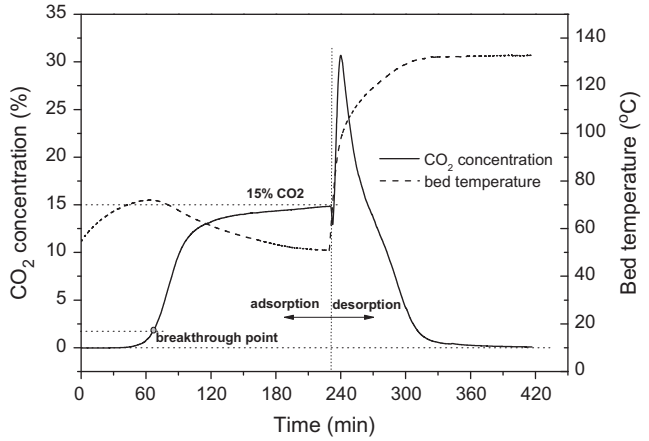

Fig. 5. Variation of CO_2 concentration and bed temperature with time during adsorption and desorption stages (Batch II).

researchers [29–32]. More CO_2 gradually escaped from the PEI–silica adsorbent bed until the detected CO_2 concentration levelled off at the input value of 15% after another 140 min. This implies that the CO_2 adsorption has slowly achieved an equilibrium condition under which PEI–silica adsorbent is saturated and cannot take any more CO_2. A desorption test was carried out immediately after the adsorbent achieved its equilibrium condition by heating the bed up to 130 °C while switching the simulated flue gas to the stripping gas of N_2 with or without the addition of moisture. The adsorbed CO_2 was quickly released during the first hour or so and the CO_2 concentration gradually dropped to zero after around 3 h. By integrating the CO_2 concentration with the gas flow rate and time, the total mass of CO_2 adsorbed during adsorption and desorbed during desorption for the given amount of adsorbent can be obtained. The capacities can then be determined as they are defined as the mass ratio of the CO_2 mass to the adsorbent mass with respect to adsorption, desorption or breakthrough point respectively. Fig. 5 also illustrates the variation of bed temperature during adsorption and desorption which will be further discussed in Section 3.7.

During an adsorption process, CO_2 molecules are physically or chemically bonded onto the surface of PEI–silica adsorbent, thus increasing the apparent mass of the bed. During a desorption process, on the contrary, the particle bed loses its mass as CO_2 is released from the surface of PEI–silica adsorbent. The change of bed mass can be verified by the variation of the pressure drop

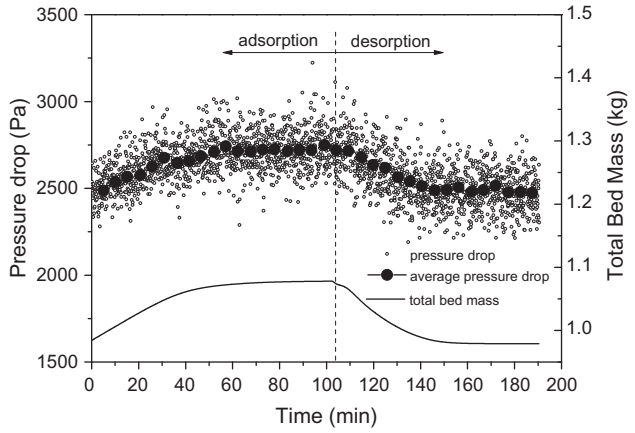

Fig. 6. Variation of pressure drop and bed mass with time during adsorption and desorption stages (Batch I).

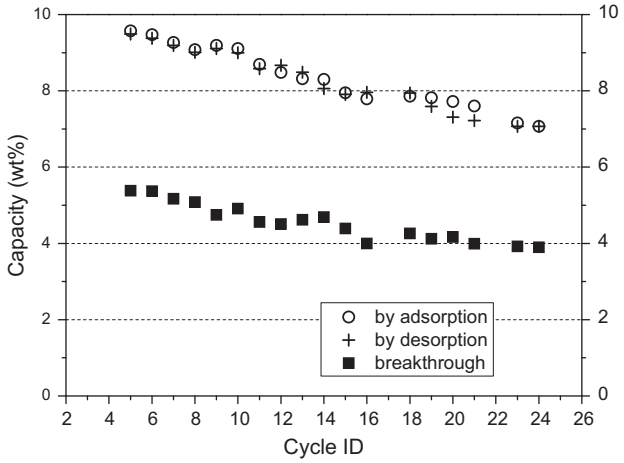

Fig. 7. Cyclic capacities of Batch I PEI–silica adsorbent (cycles ID: I5–I24, initial bed temperature 70 °C, under dry condition).

values measured by the pressure sensors. Fig. 6 illustrates how the pressure drops vary with time for Batch I PEI–silica adsorbent. Despite the fluctuation of the values in a wide range due to the nature of vibrant fluidization, the averaged pressure drops indicate a similar variation tendency as that of the total bed mass.

24 cycles of adsorption and desorption tests for Batch I PEI–silica adsorbent were carried out at an initial bed temperature of 70 °C under dry condition. The results are summarized in Fig. 7. There were no data points plotted for several cycle IDs as these cycles were conducted for other purposes such as air capture [33]. The adsorption and desorption equilibrium capacities decreased from the initial value of 9.5 wt% down to 7.0 wt% after 24 cycles. The relative loss of capacities is about 26% over 24 cycles, compared to 14% loss for TRI adsorbent over 40 cycles and 41% loss for PEI adsorbent over 22 cycles as measured by Sayari and Belmabkhout [27] under dry condition. The breakthrough capacities also showed a decreasing tendency from 5.4 wt% to 3.9 wt%. Deactivation of the adsorbent over a number of cycles is believed to be attributed to the thermal and/or oxidative degradation by the accumulated formation of urea groups [9], especially at the high desorption temperature. This feature of quick degradation is obviously unfavourable for a practical capture process as the frequency of adsorbent replacement and the operation cost can be unacceptably high.

3.3. Effect of moisture on capacities

Moisture is always present in the real flue gas stream of a power plant. Its effect on the CO_2 adsorption capacity of solid adsorbents may be minimal, detrimental or beneficial. Unlike most physisorbents such as zeolites and activated carbons [8], amine-containing sorbents, such as PEI-loaded adsorbent, are normally tolerant to the existence of moisture in the feed gas [27]. The reaction pathways between CO_2 and primary amine groups under dry and humid conditions can be described by the following schemes [34]:

$$2(RNH_2) + CO_2 \rightleftharpoons RNHCO_2^- RNH_3^+ \ (\text{carbamate}) \quad (1)$$

$$RNH_2 + CO_2 + H_2O \rightleftharpoons RNH_3^+ HCO_3^- \ (\text{bicarbonate}) \quad (2)$$

In theory, formation of bicarbonate under humid condition increases the stoichiometric CO_2/N ratio to 1.0 (indicated by Eq. (2)) from 0.5 by formation of carbamate under dry condition (indicated by Eq. (1)). However, the CO_2/N ratio can markedly deviate from the theoretical values depending on the partial pressure of

CO_2/moisture and the adsorption selectivity of CO_2 over moisture [34].

To investigate the effects of moisture on the performance of PEI–silica adsorbent, a moisture saturator is installed at the entrance of BFB to generate a stream of moisture that is introduced into the main simulated flue gas stream. The moisture saturator is operated at 40 °C and the volumetric concentration of the saturated moisture in the gas mixture is around 8.8% (wet basis). A stream of air is also introduced to the gas mixture, replacing part of the pure N_2, generating oxygen concentration at 4% (dry basis) while keeping the total dry gas flow rate at 8 l/min (at 20 °C, 1.013×10^5 Pa). The final composition of the simulated flue gas mixture (CO_2: 15% (dry basis), O_2: 4% (dry basis), balanced by N_2 with the addition of 8.8% (wet basis) moisture) represents a realistic flue gas stream from coal-fired power plants. The same amount of moisture is also present in the stripping N_2 gas flow at the desorption stage.

Fig. 8 shows the results of capacities of subsequent cycles with addition of moisture and oxygen from cycle 39 to cycle 60 (the missing cycles between cycle 25 to cycle 38 were conducted for other research purposes under dry conditions and the results haven't been included in this paper). It clearly indicates that the decreasing tendency of capacities shown in Fig. 7 has been completely avoided. The capacities were not impaired by the presence of moisture, and in the first several cycles with the presence of moisture in adsorption/desorption there was even a slight increase in capacity, probably due to the regeneration of the already degraded PEI–silica adsorbent by the aid of moisture during desorption. This finding agrees well with that obtained by Sayari and Belmabkhout [27] where the adsorption capacities stabilized over 40 cycles for three types of amine-containing adsorbents in the presence of moisture. The positive effect of moisture on the performance of PEI–silica adsorbent is utmost important as it indicates the long-term stability and low frequency of adsorbent replacement, thus making this adsorbent more competitive for commercial scale utilization.

This stabilization tendency in the capacities was also verified by using fresh Batch II PEI–silica adsorbent over 60 cycles at an initial bed temperature of 50 °C with moisture present in both adsorption and desorption stages, as illustrated in Fig. 9. Tests with absent cycle IDs (including 58–60) in Fig. 9 were conducted under different working conditions for other purposes using the same batch of adsorbent. The adsorption/desorption equilibrium capacities were stabilized at a high level of 10.6–11.1 wt% and breakthrough capacities were stabilized at around 7.6–8.2 wt%. The presence of moisture can no doubt help to alleviate the fast thermal degradation indicated in Fig. 7 but may not be able to fully compensate the thermal degradation tendency. This may be the reason why there was still a slight decrease (relatively around 5%) in capacities despite the presence of moisture in the first 23 cycles. Further degradation of the adsorbent (from cycle 27 to 57) became less significant when the moisture was always present in the stripping gas during desorption.

3.4. Effect of gas–solid contact time

The equilibrium adsorption capacity for a specific adsorbent represents the maximum adsorption capability at given working conditions. Both TGA and fluidized bed tests can reveal the similar features of reaction kinetics of CO_2 adsorption, i.e. a fast adsorption phase initially and a subsequent slow adsorption phase. The equilibrium capacity is often defined when the slow adsorption phase has completed over a relatively long period. For a typical adsorption test with Batch II adsorbent in the fluidized bed reactor, for example, it took about 1 h to reach 75% of the equilibrium capacity but more than 3 h to achieve the equilibrium capacity. During a practical capture process, the equilibrium capacity is not appropriate to be taken as the working capacity as the long adsorption time required will significantly increase the solid residence time and the inventory bed mass. The capacity at the condition when 10% of the CO_2 in the feed gas has escaped from the bed material, which corresponds to a capture rate of 90%, has been defined as the "breakthrough capacity" and regarded as the performance indicator for a practical capture process where the CO_2 concentration in the effluent gas has to be reduced to a certain level. However, TGA tests cannot determine a breakthrough capacity as the CO_2 uptake is calculated based on the mass gain of the sample but not from the CO_2 concentration in the effluent gas. The breakthrough capacity determined by our fluidized bed tests is very useful as it can be considered as the "working capacity" for a practical capture process.

The breakthrough capacities are affected by the reaction kinetics of CO_2 adsorption and the gas–solid contact time. The kinetics gives an indication of the reaction rate of CO_2 with the amine groups on or in the adsorbent surface and is affected by the characteristics of the as-prepared adsorbent such as amine type, amine loading, surface area and pore diameter of the support. For a given adsorbent, an effective measure to increase the breakthrough

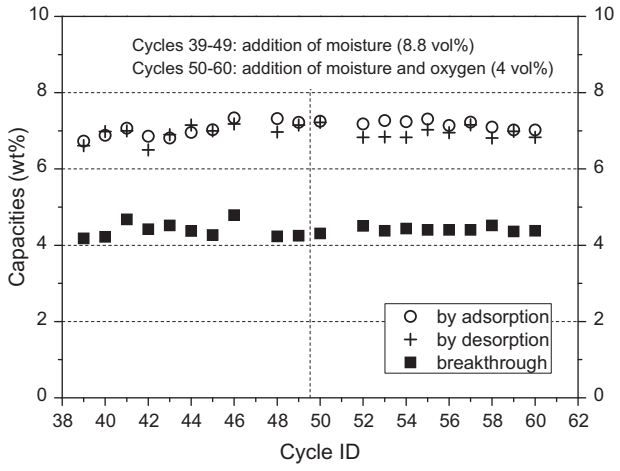

Fig. 8. Effect of moisture and oxygen in the simulated flue gas on capacities (Batch I, initial bed temperature 50 °C, cycles ID: I39–I60).

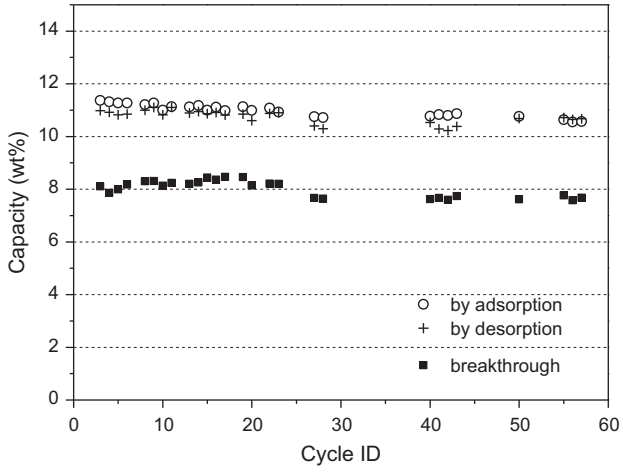

Fig. 9. Stabilization of capacities in the presence of moisture and oxygen (Batch II, initial bed temperature 50 °C, cycles ID: II1–II57).

Table 2
Comparison of capacities between Batch I and Batch II PEI–silica adsorbents.

	Mass (kg)	Bed height (m)	Gas–solid contact time (s)	Equilibrium capacities (wt%)	Breakthrough capacities (wt%)	α (–)
Batch I (fresh)	1.0	0.47	7	~9.5	~5.4	~0.56
Batch II (fresh)	1.9	0.90	13	~11.1	~8.2	~0.74

capacities is by extending the gas–solid contact time to ensure that the adsorption reaction can have sufficient time to take place.

For this purpose, Batch II adsorbent, with a nearly doubled mass compared to Batch I adsorbent, is loaded into the BFB to perform more adsorption/desorption cycles. As shown in Table 2, the gas–solid contact time has been increased from 7 s to 13 s as the bed height was increased from 0.47 m to 0.90 m. In principle, the gas–solid contact time does not affect the equilibrium capacities. The small difference in equilibrium capacities between the fresh Batch I and II adsorbents in Table 2 was mainly due to the fact that the first several Batch I tests were conducted at an initial bed temperature of 70 °C while Batch II tests were conducted at 50 °C (effect of bed temperature will be discussed in the next section). It can be seen from Table 2 that the ratio of breakthrough capacity to equilibrium capacity, denoted by α, has increased noticeably from 0.56 to 0.74 when the gas–solid contact time is increased to 13 s. The value of 0.74 implies that up to the breakthrough point the adsorbent has adsorbed 74% of the maximum amount of CO_2 that it can adsorb at the equilibrium condition.

It should be emphasized here that although an increase in gas–solid contact time can effectively increase the working capacity, it will also increase the inventory bed mass in the reactor and the reactor dimension required, thus leading to higher capital and operational costs.

3.5. Effect of adsorption temperature

Theoretically, an adsorption process of gas molecules onto the surface of a solid can be described by the Langmuir isothermal adsorption Eqs. (3) and (4) [35]:

$$\theta = \frac{q}{q_{max}} = \frac{b(T)p_{CO_2}}{1 + b(T)p_{CO_2}} = 1 - \frac{1}{1 + b(T)p_{CO_2}} \quad (3)$$

$$b(T) = b_0 \cdot \exp\left(\frac{-\Delta H_r}{RT_{ad}}\right) \quad (4)$$

where θ is a dimensionless factor indicating the fraction of the solid surface that is covered by gas molecules; q is the adsorption capacity of the solid (mol/g) while q_{max} represents the maximum adsorption capacity under the saturation condition where all surface of the solid is fully covered by one layer of gas molecules. p_{CO_2} is the partial pressure of CO_2 in the gas stream (Pa). Adsorption coefficient b (Pa^{-1}) is a function of heat of adsorption ΔH_r (kJ/kgCO_2, negative value for exothermal reaction) and adsorption temperature T_{ad} (K). b_0 is a constant in Eq. (4) (Pa^{-1}) and R is the gas constant (8.314 J/mol K). According to the Eqs. (3) and (4), the CO_2 adsorption capacity should decrease as the adsorption temperature increases, due to the exothermal nature of the adsorption process. Eq. (3) also implies the impact of the CO_2 partial pressure on the adsorption capacity. At low pressure p_{CO_2}, the value of $b(T)p_{CO_2}$ is much less than 1 so that Eq. (3) can be simplified as a linear correlation:

$$q = q_{max}b(T)p_{CO_2} \quad (5)$$

Whereas at high pressure p_{CO_2}, the value of $b(T)p_{CO_2}$ is much larger than 1 so that the value of θ can be estimated to be 1, indicating that the adsorption capacity q under high pressure equals to the maximum capacity q_{max}.

TGA experiments have been conducted to determine the CO_2 uptake at different adsorption temperatures with 15% CO_2 in N_2. The results shown in Fig. 10 indicate that CO_2 uptake is sensitive to the adsorption temperature, increasing as the temperature increases from 50 to 70 °C, reaching its peak value at around 70 °C, then decreasing as the temperature increases further to 80 °C. This observed trend does not agree with the thermodynamic behaviour implied by Langmuir Eqs. (3) and (4). Similarly, Yue et al. [36] found that the maximum adsorption capacity appeared at 100 °C for their 50 wt% TEPA-impregnated SBA-15 adsorbent. Xu et al. [37] found the maximum capacity at 75 °C for the molecular basket adsorbent and Son et al. [15] also observed a maximum capacity at 75 °C for their 50 wt% PEI-impregnated KIT-6 adsorbent. As suggested by Yue et al. [36], the appearance of the "optimal" adsorption temperature may be resulted from the compromise between diffusion-controlled effects at lower temperature and thermodynamics-controlled effects at higher temperature.

The temperature dependence on the capacities for the PEI–silica adsorbent was further investigated in the fluidized bed tests. Fig. 11 compares the adsorption capacities when the Initial Bed Temperature (IBT) was set to 50 °C and 70 °C for Batch I PEI–silica adsorbent. Due to the exothermal heat released during adsorption process, the fluidized bed temperature increased from the IBT of 50 °C and 70 °C up to about 65 °C and 80 °C respectively. Because the reactor is properly insulated and there is no cooling heat exchanger installed inside the reactor, the bed temperature would remain at the higher temperature for several hours once it was increased from the IBT. Therefore, the bed temperature with the IBT of 50 °C is closer to the optimal adsorption temperature as indicated by TGA results. The noticeable difference in capacities with two IBTs can be clearly identified from Fig. 11. For this reason, most of the adsorption tests with the BFB reactor were conducted at an IBT of 50 °C. The details of the bed temperature increase and heat of adsorption will be further discussed in Section 3.7.

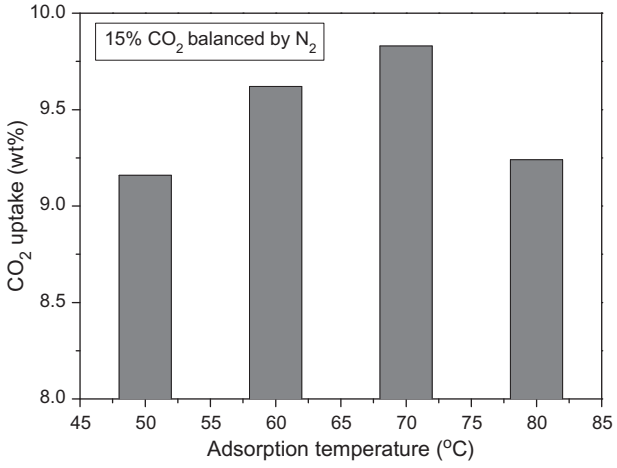

Fig. 10. TGA results of CO_2 uptake at different adsorption temperatures.

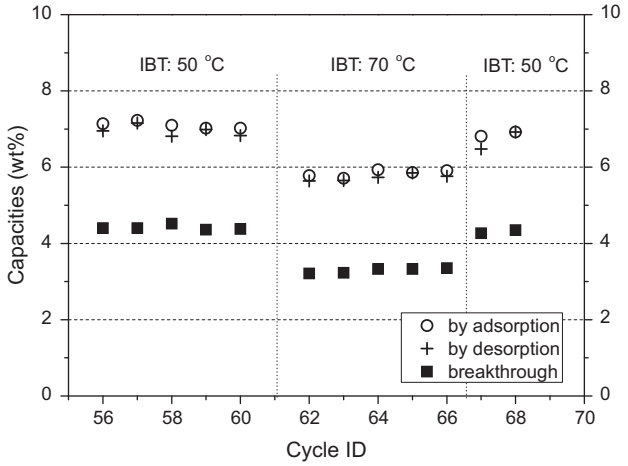

Fig. 11. Effect of initial bed temperature (IBT) on capacities (Batch I, cycles ID: I56–I68, with moisture and oxygen).

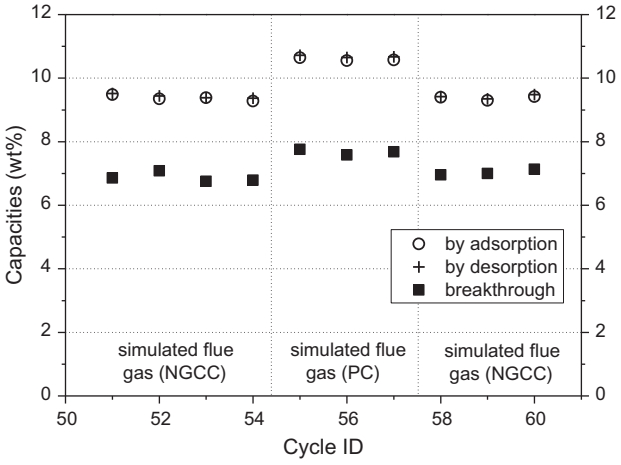

Fig. 13. Comparison of capacities for simulated flue gas from coal and natural gas-fired power plants (Batch II, initial bed temperature 50 °C, cycles ID: II51–II60).

3.6. Effect of CO_2 concentration in feed gas

One of the most advantageous features of chemi-sorbents over physi-sorbents is that chemi-sorbents do not suffer from a significant reduction in CO_2 adsorption capacities at relatively low CO_2 partial pressures. A number of tests with the BFB reactor were conducted with different CO_2 concentrations in the simulated flue gas to investigate the impact of CO_2 partial pressure. With tests II24 to II26, the CO_2 concentration in the simulated coal-fired flue gas was decreased to 5% with O_2 concentration being kept at 4% and the capacities under this condition were compared with those of the nearest cycles II20 to II23 where 15% CO_2 was present in the simulated flue gas (Fig. 12). It was expected that adsorption capacities with 5% CO_2 in the feed gas were lower than those with 15% CO_2 in the feed gas due to lower reaction kinetics. However, as illustrated in Fig. 12, the equilibrium and breakthrough capacities remained reasonably high at *ca.* 10.1 wt% and 7.7 wt% respectively, representing a relative loss of only about 8%. In order to fully simulate the flue gas of Natural Gas Combined Cycle (NGCC) power plants, the O_2 concentration in the simulated flue gas was increased to 12 vol% by replacing part of the N_2 with air while keeping the CO_2 concentration at 5%. As shown in Fig. 13, changing the simulated flue gas from the conditions of a coal-fired power plant to those of a NGCC power plant caused the adsorption capacities to reduce by a relative loss of *ca.* 11%. Capacities observed with cycles II51-54 and cycles II58-60 indicate that the high oxygen level at 12% in the simulated flue gas (NGCC) did not cause appreciable oxidative degradation. The slight difference in capacities between Figs. 12 and 13 is likely caused by the slow thermal degradation during the 24 cycles between cycle 26 and cycle 50. These results confirm that the PEI–silica adsorbent is also an efficient adsorbent for CO_2 capture from the flue gases of NGCC power plants.

Table 3 shows that the adsorption capacities of the PEI–silica adsorbent of this study are comparable to those of other PEI-based adsorbents investigated previously under a range of testing conditions. It should be noted that for the first time the adsorption capacities of a PEI–silica adsorbent have been evaluated by means of a laboratory-scale fluidized bed reactor using kg-scale adsorbent for up to 60 adsorption/desorption cycles.

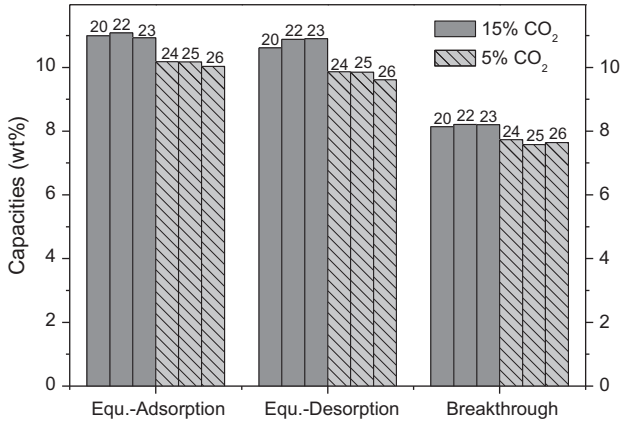

Fig. 12. Comparison of capacities when different CO_2 concentration is present in the simulated flue gas (Batch II, initial bed temperature 50 °C, cycles ID: II20–II26, numbers in figure indicate the cycle ID number).

3.7. Heat of adsorption and regeneration heat

As mentioned previously in Section 3.5, adsorption is an exothermic process with heat being released when the chemical reactions take place between CO_2 and the amine groups. For most cycles conducted in the reactor, the fluidized bed is preheated to an initial bed temperature of 50 °C before CO_2 is fed into the bed. Due to the heat released during adsorption, both the bed temperature and wall temperature would have a noticeable increase during the adsorption stage as shown in Fig. 14. More intensive reaction takes place at the lower zone of the bed due to the higher CO_2 concentration in the feed gas, leading to a higher bed temperature in this zone compared to the upper zone. There is a lag between bed and wall temperature because the thermal heat transfer between solids and wall needs a certain time to accomplish. By the time of breakthrough point, most of the heat has been released which induced a bed temperature rise of about 22–25 °C. By establishing an energy balance, the total reaction heat released equals to the sum of the heats absorbed by the gas mixture, PEI–silica adsorbent, reactor wall and the insulation material. The heat of adsorption can then be determined by dividing the accumulated heat by the accumulated amount of CO_2 that has been adsorbed until the breakthrough point. One calculation example is illustrated in Fig. 15 where accumulated heats of different components during adsorption are plotted and compared. Due to the small mass flow rate of the gas mixture, it has the least contribution to the total heat. Heat transfer from the reactor wall to the outer insulation material takes longer time owing to the high thermal conductivity of the insulation material. However, the heat absorbed

Table 3
Comparison of adsorption capacities of PEI-based solid adsorbents under different working conditions.

Support	Amine content (wt%)	CO_2 concentration (%)	Adsorption temperature (°C)	Equilibrium capacity (wt%)	Ref.
Mesoporous silica	40	15 (with 8.8% H_2O and 4% O_2)	~70	10.6–11.1	II1–II57, this study
		5 (with 8.8% H_2O and 4–12% O_2)	~70	9.4–10.1	II20–II26, II51–II60, this study
MCM-41	50	13 (with 10% H_2O, wet basis)	75	12.5	[14]
MCM-41	50	100	75	11.1	[15]
SBA-15	50	15	75	14.0	[17]
SBA-15	50	12	75	6.0	[38]
AC	30	100	25	5.0	[39]
SiO_2	40	100	60	12.3	[18]
KIT-6	50	5	75	8.6	[15]
PMMA	40	10 (with 1.2% H_2O, wet basis)	60	15.5	[16]

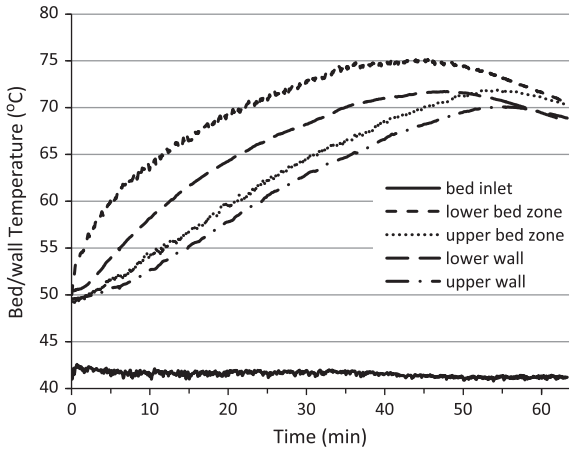

Fig. 14. Bed and wall temperature profiles during adsorption (Batch II, initial bed temperature 50 °C, breakthrough occurred at around 49 min).

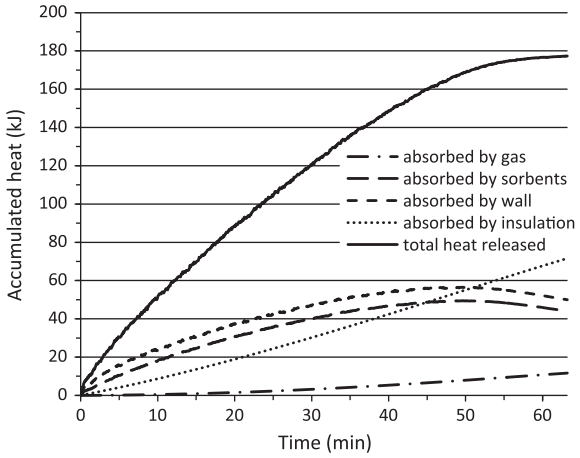

Fig. 15. Accumulated heat absorbed by different components during adsorption (Batch II, initial bed temperature 50 °C, breakthrough occurred at around 49 min).

by the insulation material becomes the largest portion after 50 min or so since the temperature gradient between outer surface of insulation material and ambient air has increased, leading to more intensive natural convection heat transfer. The calculated value of heat of adsorption is around 1870 kJ/kgCO_2 at the breakthrough point. Heat of adsorption for the fresh PEI–silica adsorbent was also measured by a SENSYS Evo TG-DSC provided by SETA-RAM® which gave the result of 2045 kJ/kgCO_2. The relative error between two methods is about 8.5%.

The energy required for the regeneration of an absorbent/adsorbent is the most important economic performance criterion for post-combustion CO_2 capture. With a reasonable degree of accuracy, the regeneration energy can be simplified to be the sum of the sensible heat that is required to heat the adsorbent from the adsorption temperature to the regeneration temperature and the latent heat (heat of adsorption) that is required to overcome the bonding energy to remove CO_2 from the adsorbent in the desorption process. The formula used to calculate the regeneration heat for a solid adsorbent is listed in Eq. (6) which is an adapted form from Hoffman et al. [40]:

$$Q_r = \frac{1}{q_w} C_{p,s}(T_{de} - T_{ad}) - \Delta H_r \quad (6)$$

where Q_r is the regeneration heat (kJ/kgCO_2 adsorbed), T_{ad} and T_{de} are the temperatures of adsorption and desorption respectively (°C), q_w is the working capacity of the adsorbent (wt%), $C_{p,s}$ is the specific heat capacity of the adsorbent (kJ/kg K), and ΔH_r is the heat of adsorption (kJ/kgCO_2 adsorbed).

The working capacity of the PEI–silica adsorbent investigated in this study is assumed to be 8 wt%, which is similar to the breakthrough capacity of Batch II adsorbent (8.2 wt%) determined by the fluidized bed tests. The specific heat capacity of the adsorbent was experimentally determined to be 1.7 kJ/kg K using a DSC III (Differential Scanning Calorimetry) device. The SENSYS Evo TG-DSC measured value of heat of adsorption, 2045 kJ/kgCO_2, is used in the calculation. By substituting these parameters into Eq. (6), the regeneration heat for the PEI–silica adsorbent in this study was calculated and compared with other amine-supported adsorbents investigated previously in Table 4.

It can be seen that the regeneration heats for all of the amine-supported sorbents in Table 4 are comparable. It should be noted that the measured value of heat of adsorption in this study is much higher than most values adopted in previous literature (e.g. 1400 kJ/kgCO_2 in [16], 1360 kJ/kgCO_2 in [42] and 1136 kJ/kgCO_2 in [18]). An adsorbent with higher heat of adsorption is expected to have higher adsorption capacity. However an increase in the

Table 4
Comparison of regeneration heats of various amine-supported sorbents.

Amine-supported sorbents	Testing conditions			Average working capacity q_w (wt%)	Regeneration heat Q_r (kJ/kgCO_2)
	Mass of sample (g)	T_{de} (°C)	Total cycles tested		
Batch II –silica adsorbent in thisstudy	1900	130	60	8	3320
Sorbent D in [41]	2.5	120	10	7.01	2600
Sorbent F in [41]	0.5	120	7	4.23	3400
Sorbent Q in [41]	0.5	130	9	3.27	3550

heat of adsorption will also increase the required regeneration heat proportionally, as implied by Eq. (6). To achieve the best economic performance for a specific CO_2 capture process with a solid adsorbent, one may need to make a compromise towards adsorption capacity so that the required regeneration heat can be minimized.

The regeneration heat for a traditional flue gas CO_2 capture process using 30 wt% MEA scrubbing technology is in the range of 3900–4500 kJ/kgCO_2 [29,43,44] on the assumption that 90% of the sensible heat can be recovered by a lean/rich solvent heat exchanger. Similarly, if we assume a conservative recovery ratio of 75% for the capture process using PEI–silica adsorbent, the required regeneration heat can then be reduced to 2360 kJ/kgCO_2, which is well below the values reported for MEA technology.

4. Conclusions

By using a laboratory-scale bubbling fluidized bed reactor loaded with a few kg solid adsorbent, the performance of the as-prepared PEI–silica adsorbent in capturing CO_2 from simulated flue gases has been evaluated. The following conclusions can be drawn from the presented experimental results and theoretical analysis:

(1) The PEI–silica adsorbent has shown typical Geldart-B bubbling fluidization behaviour and good mechanical strength and attrition resistance.
(2) The adsorption capacities for those cycles under dry condition have shown a clear degradation tendency over 24 cycles. However, the addition of moisture into the gas flow in both adsorption and desorption stages has demonstrated its ability of stabilizing the capacities. A high level of 10.6–11.1 wt% of equilibrium capacities and 7.6–8.2 wt% of breakthrough capacities over 60 cycles can be achieved under humid condition. Extension of gas–solid contact time from 7 s to 13 s can effectively improve the breakthrough capacities from 5.4 wt% to 8.2 wt% at the cost that more adsorbent needs to be loaded as the bed material.
(3) Both TGA and fluidized bed tests revealed that the adsorption capacities are sensitive to the adsorption temperature with the maximum capacity appearing at the adsorption temperature of around 70 °C.
(4) The adsorption capacities for the simulated flue gas containing 5% CO_2 are only slightly lower than those for the simulated flue gas containing 15% CO_2, implying the potential of the PEI–silica adsorbent in the application to the flue gas CO_2 capture from a NGCC power plant.
(5) The exothermal heat of adsorption is estimated to be 1870 kJ/kgCO_2 by the energy balance in the fluidized bed reactor with a relative error of 8.5% compared to the measured value by the SENSYS Evo TG-DSC (2045 kJ/kgCO_2).
(6) The calculated regeneration heat for the as-prepared PEI–silica adsorbent is found to be 3320 kJ/kgCO_2 which is comparable to other reported amine-based solid sorbents. This energy penalty can be further reduced to 2360 kJ/kgCO_2 if 75% of sensible heat recovery can be realized by proper process design, which is well below the values of 3900–4500 kJ/kgCO_2 for a traditional MEA scrubbing process with 90% recovery of sensible heat.

The results obtained so far in this study have indicated that the as-prepared PEI–silica adsorbent is a good candidate for post-combustion carbon capture from both coal and natural gas-fired power plants. However, further research on the long-term (much more than 60 cycles) stability and regeneration strategies of the adsorbent is still needed.

Acknowledgements

The authors wish to acknowledge the financial support of UK EPSRC (EP/J020745/1, EP/G063176/1) and Miss. Jingjing Liu's help with TGA measurements and SEM analyses.

References

[1] International Energy Agency (IEA), World Energy Outlook (WEO), Special Report: Redrawing the Energy-Climate Map (2013). <http://www.iea.org/media/freepublications/2013pubs/WEO2013_Climate_Excerpt_ES_WEB.pdf> (accessed 26.01.14).
[2] U.S. Energy Information Administration (EIA), International Energy Outlook (2013). <http://www.eia.gov/forecasts/ieo/world.cfm> (accessed 26.01.14).
[3] D. Bonenfant, M. Kharoune, P. Niquette, M. Mimeault, R. Hausler, Advances in principle factors influencing carbon dioxide adsorption on zeolites, Sci. Technol. Adv. Mater. 9 (2008) 013007.
[4] C. Lu, H. Bai, B. Wu, F. Su, J.F. Hwang, Comparative study of CO_2 capture by carbon nanotubes, activated carbons, and zeolites, Energy Fuels 22 (2008) 3050–3056.
[5] F. Su, C. Lu, S.C. Kuo, W. Zeng, Adsorption of CO_2 on amine-functionalized Y-type zeolites, Energy Fuels 24 (2010) 1441–1448.
[6] R.V. Siriwardane, M.S. Shen, E.P. Fisher, J.A. Poston, Adsorption of CO_2 on molecular sieves and activated carbon, Energy Fuels 15 (2001) 279–284.
[7] M.G. Plaza, C. Pevida, B. Arias, Different approaches for the development of low-cost CO_2 adsorbents, J. Environ. Eng. 135 (2009) 426–432.
[8] Y. Belmabkhout, A. Sayari, Effect of pore expansion and amine functionalization of mesoporous silica on CO_2 adsorption over a wide range of conditions, Adsorption 15 (2009) 318–328.
[9] T.C. Drage, A. Arenillas, K.M. Smith, C.E. Snape, Thermal stability of polyethyleneimine based carbon dioxide adsorbents and its influence on selection of regeneration strategies, Microporous Mesoporous Mater. 116 (2008) 506–512.
[10] J.C. Hicks, J.H. Drese, D.J. Fauth, M.L. Gray, G. Qi, C.W. Jones, Designing adsorbents for CO_2 capture from flue gas – hyperbranched aminosilicas capable of capturing CO_2 reversibility, J. Am. Chem. Soc. 130 (2008) 2902–2903.
[11] S. Choi, J.H. Drese, C.W. Jones, Adsorbent materials for carbon dioxide capture from large anthropogenic point sources, ChemSusChem 2 (2009) 796–854.
[12] A.O. Yazaydin, R.Q. Snurr, T.H. Park, K. Koh, J. Liu, Screening of metal–organic frameworks for carbon dioxide capture from flue gas using a combined experimental and modelling approach, J. Am. Chem. Soc. 131 (2009) 18198–18199.
[13] J. An, S.J. Geib, N.L. Rosi, Highly selective CO_2 uptake in acobalt adeninate metal–organic framework exhibiting pyrimidine and amino-decorated pores, J. Am. Chem. Soc. 132 (2010) 38–39.
[14] X. Xu, C. Song, B.G. Miller, A.W. Scaroni, Influence of moisture on CO_2 separation from gas mixture by a nanoporous adsorbent based on polyethyleneimine-modified molecular sieve MCM-41, Ind. Eng. Chem. Res. 44 (2005) 8113–8119.
[15] W.J. Son, J.K. Choi, W.S. Ahn, Adsorptive removal of carbon dioxide using polyethyleneimine-loaded mesoporous silica materials, Microporous Mesoporous Mater. 113 (2008) 31–40.
[16] M.L. Gray, J.S. Hoffman, D.C. Hreha, D.J. Fauth, S.W. Hedges, K.J. Champagne, H.W. Pennline, Parametric study of solid amine sorbents for the capture of carbon dioxide, Energy Fuels 23 (2009) 4840–4844.
[17] X. Ma, X. Wang, C. Song, Molecular basket sorbents for separation of CO_2 and H_2S from various gas streams, J. Am. Chem. Soc. 131 (2009) 5777–5783.
[18] A.D. Ebner, M.L. Gray, N.G. Chisholm, Q.T. Black, D.D. Mumford, M.A. Nicholson, J.A. Ritter, Suitability of a solid amine sorbent for CO_2 capture by pressure swing adsorption, Ind. Eng. Chem. Res. 50 (2011) 5634–5641.
[19] V. Nikulshina, M.E. Galvez, A. Steinfeld, Kinetic analysis of the carbonzation reactions for the capture of CO_2 from air via the $Ca(OH)_2$–$CaCO_3$–CaO solar thermochemical cycle, Chem. Eng. J. 129 (2007) 75–83.
[20] F. Zeman, Experimental results for capturing CO_2 from the atmosphere, AIChE J. 54 (2008) 1396–1399.
[21] J. Blamey, D.Y. Lu, P.S. Fennell, E.J. Anthony, Reactivation of CaO-based sorbents for CO_2 capture: mechanism for the carbonation of $Ca(OH)_2$, Ind. Eng. Chem. Res. 50 (2011) 10329–10334.
[22] G. Montes-Hernandez, R. Chiriac, F. Toche, F. Renard, Gas–solid carbonation of $Ca(OH)_2$ and CaO particles under non-isothermal and isothermal conditions by using a thermogravimetric analyzer: implications for CO_2 capture, Int. J. Greenhouse Gas Control 11 (2012) 172–180.
[23] W.-C. Yang, Handbook of Fluidization and Fluid-Particle Systems, CRC Press, 2003.
[24] S. Sjostrom, H. Krutka, T. Starns, T. Campbell, Pilot test results of post-combustion CO_2 capture using solid sorbents, Energy Proc. 4 (2011) 1584–1592.
[25] R. Veneman, Z.S. Li, J.A. Hogendoorn, S.R.A. Kersten, D.W.F. Brilman, Continuous CO_2 capture in a circulating fluidized bed using supported amine sorbents, Chem. Eng. J. 207–208 (2012) 18–26.
[26] T.C. Drage, A. Arenillas, K.M. Smith, C. Pevida, S. Piippo, C.E. Snape, Preparation of carbon dioxide adsorbents from the chemical activation of urea-formaldehyde and melamine-formaldehyde resins, Fuel 86 (2007) 22–31.

[27] A. Sayari, Y. Belmabkhout, Stabilization of amine-containing CO_2 adsorbents: dramatic effect of water vapor, J. Am. Chem. Soc. 132 (2010) 6312–6314.
[28] W. Li, S. Choi, J.H. Drese, M. Hornbostel, G. Krishnan, P.M. Eisenberger, C.W. Jones, Steam-stripping for regeneration of supported amine-based CO_2 adsorbents, ChemSumChem 3 (2010) 899–903.
[29] M.R.M. Abu-Zahra, L.H.J. Schneiders, J.P.M. Niederer, P.H.M. Feron, G.F. Versteeg, CO_2 capture from power plants, Part I. A parametric study of the technical performance based on monoethanolamine, Int. J. Greenhouse Gas Control. 1 (2007) 37–46.
[30] W.C. Yang, J. Hoffman, Exploratory design study on reactor configurations for carbon dioxide capture from conventional power plants employing regenerable solid sorbents, Ind. Eng. Chem. Res. 48 (2009) 341–351.
[31] G.D. Pirngruber, F. Guillou, A. Gomez, M. Clausse, A theoretical analysis of the energy consumption of post-combustion CO_2 capture processes by temperature swing adsorption using solid sorbents, Int. J. Greenhouse Gas Control. 14 (2013) 74–83.
[32] R. Veneman, H. Kamphuis, D.W.F. Brilman, Post-combustion CO_2 capture using supported amine sorbents: a process integration study, Energy Proc. 37 (2013) 2100–2108.
[33] W. Zhang, H. Liu, C. Sun, T.C. Drage, C.E. Snape, Capturing CO_2 from ambient air using a polyethyleneimine–silica adsorbent in fluidized beds, Chem. Eng. Sci. (2014). in press.
[34] R. Serna-Guerrero, Y. Belmabkhout, A. Sayari, Influence of regeneration conditions on the cyclic performance of amine-grafted mesoporous silica for CO_2 capture: an experimental and statistical study, Chem. Eng. Sci. 65 (2010) 4166–4172.
[35] I. Langmuir, The constitution and fundamental properties of solids and liquids. Part I. solids, J. Am. Chem. Soc. 38 (1916) 2221–2295.
[36] M.B. Yue, Y. Chun, Y. Cao, X. Dong, J.H. Zhu, Novel CO_2-capturer derived from the as-prepared SBA-15 occluded by template, Adv. Funct. Mater. 16 (2006) 1717–1722.
[37] X. Xu, C. Song, J.M. Andresen, B.G. Miller, A.W. Scaroni, Novel polyethylenimine-modified mesoporous molecular sieve of MCM-41 type as high-capacity adsorbent for CO_2 capture, Energy Fuels 16 (2002) 1463–1469.
[38] S. Dasgupta, A. Nanoti, P. Gupta, D. Jena, A.N. Goswami, M.O. Garg, Carbon dioxide removal with mesoporous adsorbents in a single column pressure swing adsorber, Sep. Sci. Technol. 44 (2009) 3973–3983.
[39] M.G. Plaza, C. Pevida, A. Arenillas, F. Rubiera, J.J. Pis, CO_2 capture by adsorption with nitrogen enriched carbons, Fuel 86 (2007) 2204–2212.
[40] J.S. Hoffman, G.A. Richards, H.W. Pennline, D. Fischer, G. Keller, Factors in reactor design for carbon dioxide capture with solid, regenerable sorbents, in: Clearwater Coal Conference, Clearwater, FL, 2008.
[41] S. Sjostrom, H. Krutka, Evaluation of solid sorbents as a retrofit technology for CO_2 capture, Fuel 89 (2010) 1298–1306.
[42] A.H. Berger, A.S. Bhown, Comparing physisorption and chemisorption solid sorbents for use separating CO_2 from flue gas using temperature swing adsorption, Energy Proc. 4 (2011) 562–567.
[43] T.J. Tarka, J.P. Ciferno, M.L. Gray, D. Fauth, CO_2 capture systems using amine enhanced solid sorbents, in: Proceedings of the 5th Annual Conference on Carbon Capture and Sequestration, Pittsburg, PA, 2006.
[44] A.B. Rao, E.S. Rubin, D.W. Keith, M.G. Morgan, Evaluation of potential cost reductions from improved amine-based CO_2 capture systems, Energy Policy 34 (2006) 3765–3772.